Management of Wind Power Variations in Electricity System Investment Models. A Parallel Computing Strategy

SN Oper. Res. Forum (2021) 2: 25
https://doi.org/10.1007/s43069-021-00065-0

ORIGINAL RESEARCH

Management of Wind Power Variations in Electricity System Investment Models

A Parallel Computing Strategy

Lisa Göransson[1] · **Caroline Granfeldt**[2] · **Ann-Brith Strömberg**[2]

Received: 22 October 2020 / Accepted: 8 April 2021 / Published online: 4 May 2021

Abstract
Accounting for variability in generation and load and strategies to tackle variability cost-efficiently are key components of investment models for modern electricity systems. This work presents and evaluates the Hours-to-Decades (H2D) model, which builds upon a novel approach to account for strategies to manage variations in the electricity system covering several days, the variation management which is of particular relevance to wind power integration. The model discretizes the time dimension of the capacity expansion problem into 2-week segments, thereby exploiting the parallel processing capabilities of modern computers. Information between these segments is then exchanged in a consensus loop. The method is evaluated with regard to its ability to account for the impacts of strategies to manage variations in generation and load, regional resources and trade, and inter-annual linkages. Compared to a method with fully connected time, the proposed method provides solutions with an increase in total system cost of no more than 1.12%, while reducing memory requirements to 1/26'th of those of the original problem. For capacity expansion problems concerning two regions or more, it is found that the H2D model requires 1–2% of the calculation time relative to a model with fully connected time when solved on a computer with parallel processing capability.

Keywords Flexibility measures · Variation management · Electricity system model · Capacity expansion model · Parallel computing · Hours-to-Decades model · Wind power integration · Consensus algorithm

1 Introduction

Given that the electricity system is undergoing a major transition, methods and models applied to assess investments in and operation of the electricity system must be adapted to capture the essential features of the electricity system in transition

✉ Lisa Göransson
lisa.goransson@chalmers.se

Extended author information available on the last page of the article

as well as the properties of new electricity systems coming online. A major driver for change in the electricity system is the effort to produce electricity without emitting carbon dioxide, so as to mitigate climate change. Wind power and solar power offer electricity that is associated with low or no emissions of carbon dioxide, and are also expected to be the most affordable electricity generation options in many parts of the world from 2040 and onwards [1]. For the locations where wind and solar power offer electricity at a lower cost relative to other options, the variability of wind and solar power generation is a key limiting factor for the shares of the electricity demand supplied by wind and solar power. Therefore, for electricity system investment models that examine future electricity system compositions, it is crucial to account for this variability [2, 3].

The most straightforward means to include variability in electricity system models is to adopt a high time resolution. However, electricity system investment models addressing the capacity expansion problem typically cover at least the 40 years a thermal power plant is in operation. Thus, an hourly time resolution implies that each type of generation technology in each region considered introduces 40×8760 variables. If thermal cycling is accounted for the number of variables representing electricity generation is doubled [4]. In order to reduce the computer memory requirements and computation time, long-term electricity system models therefore typically adopt some kind of simplified time representation. In a review of modelling tools for energy and electricity systems with large shares of variable renewable electricity (VRE) [5], the representation of short-term variability in long-term studies is identified as a key remaining challenge. In a methodological review of strategies to integrating short-term variations of the power system into integrated energy system models, the traditional ways to representing time in long-term energy system optimization models are discussed relative proposed approaches for improved time representation [6]. The authors build on the work by [7], stating that the typical stylized temporal representation in long-term energy system optimization models is in the form of a low number of integral or semi-dynamic time-slices, where integral time-slices represent average load levels during certain fractions of the year, while semi-dynamic time-slices represent typical or representative fractions of the year. Four distinct approaches to improve time representation in long-term energy system models are identified: 1) semi-dynamic balancing using typical days with increased resolution, 2) integral balancing based on approximating the joint probability distribution of the load and VRE generation, 3) semi-dynamic balancing using representative historical periods, and 4) using stochastic programming as a means to address modelling uncertainties. Time-slicing methods using integral balancing based on approximating the joint probability distribution of the load and VRE generation are developed by, for example, Wogrin et al. [8] (i.e., the system state method) and Lehtveer et al. [9]. Nahmmacher et al. [10] propose a method to reduce the size of the time representation, which is based on semi-dynamic balancing using representative historical periods, i.e., the identification of a number of days (24-hour segments) taken to represent the year. This method is referred to as the *representative days* approach. The choice of segments is based on the load, wind, and solar patterns over 24 hours. Both of the time reduction methods, as developed in [8] and [10], respectively, have been shown to satisfactorily represent variability in long-term electricity system models, and several investment models

have been updated in line with these or similar principles (see [11–14]). The performance of integral balancing based on approximating the joint probability distribution of the load and VRE generation, and semi-dynamic balancing using representative historical periods, has been compared using an hourly unit commitment model as benchmark (see [15]).

Challenges remain, however, for long-term investment models to assess electricity systems with large shares of varying renewables. One challenge for integral balancing based on approximating the joint probability distribution of the load and VRE generation is that, in difference to load variations, variations in wind and solar generation do *not* follow a common pattern across a wide geographical scope. Thus, in models with a large geographical coverage, integral time-slicing which account for wind and solar variations cannot be adopted while considering energy balances on subregional level representing limitations in transmission capacity [16]. The inclusion of strategies to manage variations poses additional challenges on the electricity system models, as the implementation of strategies to manage variations, e.g., the state of an energy storage or thermal power plant, connects time sequences. While capturing the impact of flexibility provision within the time-slice of semi-dynamic balancing using representative historical days is straightforward with the representative days approach, wind variation management over longer time periods requires substantial additions to the original method [17] increasing calculation times and complexity.

This work proposes a heuristic modeling methodology designed with these challenges in mind, i.e., a model structured to accommodate strategies to manage wind power variations as well as transmission limitations. Brown et al. [18] avoid reducing the time dimension by reducing the number of technologies included, excluding thermal generation with limited flexibility such as nuclear power and steam plants. The method proposed in this work suggests a heuristic approach to the capacity expansion problem with emphasis on strategies to manage wind variations, including thermal cycling as well as transmission and trade. The method accounts for every third hour of the year while including thermal generation and considers thermal cycling by decomposing the capacity expansion problem into 26 2-week segments, adopted to wind variation with typical duration of several days [19]. The 2-week segments are solved in parallel, and a consensus loop gathers information from the initial solves and uses this information to form one capacity–cost curve for each technology and region, which form the basis for subsequent iterations. An iteration is in this work defined as parallel solves of the capacity expansion problem and formation of a capacity–cost curve based on the results. The decomposed problem is iterated until consensus is attained, and storage and transmission capacity no longer change between iterations. The model developed based on this methodology is referred to as the *Hours-to-Decades* (H2D) model and is of particular relevance for large interconnected regions with good conditions for wind power such as Europe. The method shares elements with mathematical decomposition methods, such as Lagrangian decomposition [20], where an optimization problem is decomposed into smaller subproblems that can be solved in parallel. An iterative loop, as, for example, a subgradient [21] or bundle [22] method, applied to a dual problem [23]—here corresponding to the consensus loop—is then used to reach an optimal solution to the original problem.

2 Methodology

The H2D model developed in this work consists of two main parts: *a decomposed electricity system investment model* and a *consensus loop* that enables the exchange of information between 2-week segments of the electricity system model. Figure 1 presents a schematic illustration of the modelling methodology.

The electricity system model represents the problem of meeting the demand for electricity while minimizing investment and operational costs for 26 separate 2-week segments. In the consensus loop, information from the solutions is gathered in capacity–cost curves in which the capacity invested in all 2-week segments has the lowest cost, while additional capacity invested in a subset of the segments is more expensive; further on, the smaller the subset of segments, the more expensive the capacity. The solution process is iterated until there is consensus, i.e., the capacity–cost curves are unchanged between iterations. This section provides a mathematical description of the investment model and the consensus loop followed by a description of the approach applied to connect years when investigating pathways for the electricity system. The section ends by outlining the method applied to evaluate the proposed modeling methodology.

2.1 Electricity System Investment Model

The electricity system investment model identifies investments in electricity generation and storage technologies such that the demand for electricity can be met at the lowest cost. It is a linear, cost-minimizing model that is designed to account for variability and accommodate strategies to manage variations in the hourly to weekly timescale. Chronology in time is maintained using 2-week segments, enabling the inclusion of thermal cycling and storage with hourly-to-weekly cycles, so as to represent the system responses to wind variations. Segments of full weeks have the advantage of capturing variations in electricity demand between day and night as well as workday and weekend. To maximize the usage of parallel computation capacity of modern computers, as short segments as possible are desired. However, one-week segments are too short to fully capture the wind power variability, for which a persistence of 8 days is common on a hub height of 100m [24]. The advantage of two-week segments was confirmed in preliminary tests using one-week and four-week segments. In this work, the 2-week segments have a 3-hour time resolution. Seasonal variability is represented by accounting for all the 2-week segments in a year. However, dimensioning of seasonal storage (i.e., storages shifting electricity from summer to winter or vice versa) is not possible with this approach; the implications of this are considered in the discussion, Sect. 4. The model includes thermal cycling as well as battery and hydrogen storage. Hydrogen storage investments are stimulated by introducing a demand for electricity in hydrogen production for industry corresponding to 20% of the annual electricity demand evenly distributed over the year.

All notations used in the electricity system model developed below are described in the nomenclature list provided in Appendix A, Tables 4, 5, and 6, in which also nonnegativity constraints—as applicable—of the variables are indicated. In order to simplify the presentation, the years modelled are omitted in the relations (1)–(21).

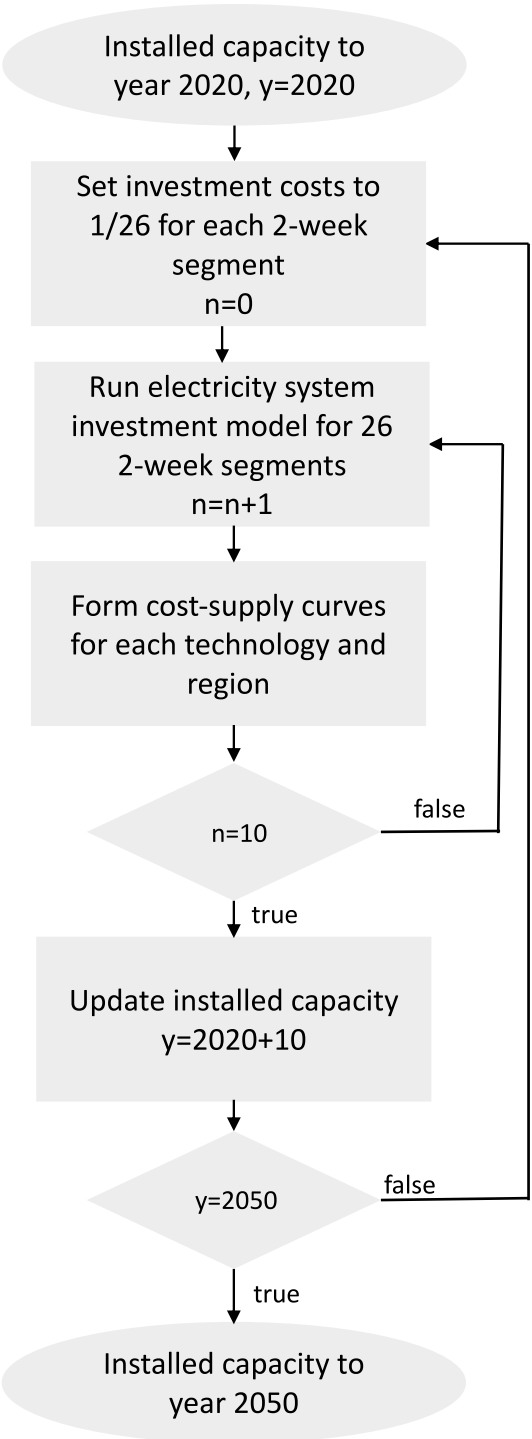

Fig. 1 A schematic illustration of the modelling methodology

For each 2-week segment $s \in \mathcal{S}$, the objective function to be minimized is expressed as

$$c_s^{\text{tot}} := \sum_{i\in\mathcal{I}} \sum_{p\in\mathcal{P}} \sum_{r\in\mathcal{R}} C_p^{\text{inv}} \lambda_{iprs}^{\text{e}} w_{ipr} \tag{1}$$

$$+ \sum_{i\in\mathcal{I}} \sum_{p\in\mathcal{P}} \sum_{t\in\mathcal{T}_s} \left(C_{pt}^{\text{run}} g_{ipt} + c_{ipt}^{\text{cycl}} \right) \tag{2}$$

$$+ \sum_{i\in\mathcal{I}} \sum_{q\in\mathcal{Q}} \sum_{j\in\mathcal{I}\setminus\{i\}} \sum_{r\in\mathcal{R}} C_q^{\text{h-inv}} \lambda_{ijqrs}^{\text{h}} h_{ijqr} \tag{3}$$

$$+ \sum_{i\in\mathcal{I}} \sum_{j\in\mathcal{I}\setminus\{i\}} \sum_{t\in\mathcal{T}_s} C_t^{\text{exp}} e_{jit}^{\text{pos}}, \tag{4}$$

where (1) represents the costs for investments in the different technologies in the different regions, (2) the running costs of the different technologies in the different regions at all time steps within the 2-week segment, (3) the costs for investments in technologies for transmission of electricity between the regions, and (4) the costs of transmitting electricity between the regions in each time step within the 2-week segment.

Let w_{ipr} denote the installed capacity in technology p, in region i and cost class r, and let h_{ijqr} denote the installed transmission capacity between regions i and j, using transmission technology q in cost class r. The investments in each cost class have to stay below the cost class potentials, M_{ipr}^{e} and M_{ijqr}^{h}, respectively (computed by the consensus loop described in Sect. 2.2), which is modelled by the inequalities

$$w_{ipr} \le M_{ipr}^{\text{e}}, \qquad i \in \mathcal{I},\ p \in \mathcal{P},\ r \in \mathcal{R}, \tag{5}$$

$$h_{ijqr} \le M_{ijqr}^{\text{h}}, \qquad i \in \mathcal{I},\ j \in \mathcal{I},\ q \in \mathcal{Q},\ r \in \mathcal{R}. \tag{6}$$

Let d_{it}^{hydrogen} denote the electricity consumption of the electrolyzer, let e_{ijt} denote the electricity exported from region i to region j in time step t, and let b_{ipt}^{charge} and $b_{ipt}^{\text{discharge}}$ denote the charging and discharging, respectively, of battery technology p in region i and time step t. The demand for electricity, D_{it}, must be met in all regions at all times, which then implies the inequalities

$$\sum_{p\in\mathcal{P}^{\text{gen}}} g_{ipt} \ge D_{it} + d_{it}^{\text{hydrogen}} + \sum_{j\in\mathcal{I}\setminus\{i\}} e_{ijt} + \sum_{p\in\mathcal{P}^{\text{bat}}} \left(b_{ipt}^{\text{charge}} - b_{ipt}^{\text{discharge}} \right), \quad i \in \mathcal{I},\ t \in \mathcal{T}_s,\ s \in \mathcal{S}. \tag{7}$$

The import and the export of electricity are required to be balanced, and the export may not exceed the installed transmission capacity, as expressed by the relations

$$-e_{ijt} = e_{jit} \leq \sum_{j \in \mathcal{I} \setminus \{i\}} \sum_{q \in \mathcal{Q}} \sum_{r \in \mathcal{R}} h_{ijqr}, \quad i \in \mathcal{I},\ j \in \mathcal{I},\ t \in \mathcal{T}_s,\ s \in \mathcal{S}, \tag{8}$$

$$e^{\text{pos}}_{ijt} = |e_{ijt}| = \max\{e_{ijt}, e_{jit}\}, \quad i \in \mathcal{I},\ j \in \mathcal{I},\ t \in \mathcal{T}_s,\ s \in \mathcal{S}. \tag{9}$$

The level of generation may not exceed the installed capacity weighted by the profile $\theta_{ipt} \in [0, 1]$, which is weather-dependent for wind and solar power, but equals 1 for all $p \in \mathcal{P}^{\text{therm}}$:

$$g_{ipt} \leq \sum_{r \in \mathcal{R}} w_{ipr} \theta_{ipt}, \quad i \in \mathcal{I},\ p \in \mathcal{P},\ t \in \mathcal{T}_s,\ s \in \mathcal{S}. \tag{10}$$

Flow batteries and lithium ion batteries are amongst the investment options in the model. For each storage, an energy balance constraint controls its state. Further, the storage level, g_{ipt}, the charging, $\eta_p b^{\text{charge}}_{ipt}$, and the discharging, $b^{\text{discharge}}_{ipt}$, of the battery during the last time step of each 2-week segment s, constrain the battery storage level in the first time step of the same 2-week segment, where η_p denotes the efficiency of technology p:

$$g_{ipt} + \eta_p b^{\text{charge}}_{ipt} - b^{\text{discharge}}_{ipt} \geq \begin{cases} g_{i,p,t+1}, & t \in \mathcal{T}_s \setminus \{sT\}, \\ g_{i,p,t-(T-1)}, & t = sT, \end{cases} \quad i \in \mathcal{I},\ p \in \mathcal{P}^{\text{bat}},\ s \in \mathcal{S}. \tag{11}$$

The charging and discharging of batteries may not exceed the installed battery storage capacity, assuming a maximum C-rate of 1 ("1C rate" corresponds to the charge/discharge current that will charge/discharge the entire battery in one hour):

$$b^{\text{charge}}_{ipt} \leq \sum_{r \in \mathcal{R}} w_{ipr}, \quad i \in \mathcal{I},\ p \in \mathcal{P}^{\text{bat}},\ t \in \mathcal{T}_s,\ s \in \mathcal{S}, \tag{12}$$

$$b^{\text{discharge}}_{ipt} \leq \sum_{r \in \mathcal{R}} w_{ipr}, \quad i \in \mathcal{I},\ p \in \mathcal{P}^{\text{bat}},\ t \in \mathcal{T}_s,\ s \in \mathcal{S}. \tag{13}$$

For the cases including hydrogen demand and hydrogen storage, there is a balance inequality assuring that the demand, D^{hydrogen}_i, for hydrogen from industry is met by hydrogen production, $\eta_p d^{\text{hydrogen}}_{it}$, in the electrolyzer. Further, the storage level, and the charging and discharging of the hydrogen storage during the last time step of the 2-week segment are used to constrain the hydrogen storage level in the first time step of the same 2-week segment. Letting η_p denote the efficiency of charging the hydrogen storage, this is modelled as

$$g_{ipt} + \eta_p d^{\text{hydrogen}}_{it} - D^{\text{hydrogen}}_i \geq \begin{cases} g_{i,p,t+1}, & t \in \mathcal{T}_s \setminus \{sT\}, \\ g_{i,p,t-(T-1)}, & t = sT, \end{cases} \quad i \in \mathcal{I},\ p \in \mathcal{P}^{\text{hydrogen}},\ s \in \mathcal{S}. \tag{14}$$

The electricity consumption of the electrolyzer, d^{hydrogen}_{it}, may not exceed the installed electrolyzer capacity:

$$d_{it}^{\text{hydrogen}} \leq \sum_{r \in \mathcal{R}} w_{ipr}, \quad i \in \mathcal{I},\ p \in \mathcal{P}^{\text{electrolysis}},\ t \in \mathcal{T}_s,\ s \in \mathcal{S}. \tag{15}$$

Wind power sites are ordered in classes. Offshore sites are represented by one class, while onshore sites are organized into several classes corresponding to different wind conditions. Each class is represented as one generation technology $p \in \mathcal{P}^{\text{wind}}$. Investments in wind power capacity cannot exceed the regional resources for the respective technology, A_{ip}, according to

$$\sum_{r \in \mathcal{R}} w_{ipr} \leq A_{ip}, \quad i \in \mathcal{I},\ p \in \mathcal{P}^{\text{wind}}. \tag{16}$$

For solar power, there is a total resource constraint for each modeled region i:

$$\sum_{r \in \mathcal{R}} \sum_{p \in \mathcal{P}^{\text{solar}}} w_{ipr} \leq \sum_{p \in \mathcal{P}^{\text{solar}}} A_{ip}, \quad i \in \mathcal{I}. \tag{17}$$

Previous work has shown that the inclusion of thermal cycling has a substantial impact on the cost-optimal electricity system composition [25]. Thermal cycling is here accounted for by applying the relaxed unit commitment approach suggested by [26] and evaluated relative to the full-unit commitment by one of the authors in [4]. With this approach, the variables g_{ipt}^{active} represent the capacity that is active and available for generation in each time-step t, in each region $i \in \mathcal{I}$, and within each technology aggregate $p \in \mathcal{P}^{\text{therm}}$. Further, the level of generation may not be below the *minimum load share*, $\xi_p^{\min}$, of the active capacity, g_{ipt}^{active}, for the technology aggregate. These relations are modelled by the inequalities

$$\xi_p^{\min} g_{ipt}^{\text{active}} \leq g_{ipt} \leq g_{ipt}^{\text{active}}, \qquad i \in \mathcal{I},\ p \in \mathcal{P}^{\text{therm}},\ t \in \mathcal{T}_s,\ s \in \mathcal{S}. \tag{18}$$

The amount of capacity started in each time step is controlled by the variables g_{ipt}^{on}. In each time step, the active capacity is limited by the sum of the capacity started and the active capacity in the previous time step. However, for the first time step of each 2-week segment, except the first segment, the active capacity in the previous time step is represented by the active capacity in the last time step of the previous segment, as given by the previous iteration of the consensus loop (see Sect. 2.2), i.e., by $G_{i,p,t-1}^{\text{active}}$. Further, for the first time step of the first segment (i.e., for $t = 1$), the active capacity in the last time step of the last segment is used, as given by the previous iteration of the consensus loop, i.e., by $G_{i,p,ST}^{\text{active}}$. These relations are modelled by the inequalities

$$g_{ipt}^{\text{active}} \leq g_{ipt}^{\text{on}} + \begin{cases} g_{i,p,t-1}^{\text{active}}, & t \in \mathcal{T}_s \setminus \{(s-1)T+1\}, \quad s \in \mathcal{S}, \\ G_{i,p,t-1}^{\text{active}}, & t = (s-1)T+1, \qquad\quad s \in \mathcal{S} \setminus \{1\}, \qquad i \in \mathcal{I},\ p \in \mathcal{P}^{\text{therm}}. \\ G_{i,p,ST}^{\text{active}}, & t = 1, \end{cases} \tag{19}$$

The start-up cost is proportional to the started capacity g_{ipt}^{on}, while the part-load cost is proportional to the difference between the active generation capacity and the generation level. To avoid boundary effects, a value for the thermal generation in

operation during the last time step of the 2-week segment is applied that is proportional to the start-up cost paid in the first hour of the 2-week segment, based on the started capacity, $G^{\text{on}}_{i,p,sT+1}$, and the active capacity, $G^{\text{active}}_{i,p,sT+1}$, in the first hour of the next segment, as given by the solution to the previous iteration. For each $i \in \mathcal{I}$ and $p \in \mathcal{P}^{\text{therm}}$, these constraints are expressed as

$$c^{\text{cycl}}_{ipt} \geq C^{\text{on}}_{ipt} g^{\text{on}}_{ipt} + C^{\text{part}}_{ipt}\left(g^{\text{active}}_{ipt} - g_{ipt}\right) - \frac{g^{\text{active}}_{ipt}}{2} \cdot \begin{cases} 0, & t \in \mathcal{T}_s \setminus \{sT\}, \quad s \in \mathcal{S}, \\ \frac{C^{\text{on}}_{i,p,t+1} G^{\text{on}}_{i,p,t+1}}{G^{\text{active}}_{i,p,t+1}}, & t = sT, \qquad\quad s \in \mathcal{S} \setminus \{S\}, \\ \frac{C^{\text{on}}_{ip1} G^{\text{on}}_{ip1}}{G^{\text{active}}_{ip1}}, & t = ST. \end{cases} \tag{20}$$

Hence, if thermal capacity is active in the end of one 2-week segment and also in the beginning of the subsequent 2-week segment, the start-up cost for that capacity is shared equally between segments. Thermal generation is subject to a start-up time, i.e., it takes some time for a thermal power plant to heat up before it can deliver electricity. Thus, in the model, once capacity is deactivated, it cannot become active again during the interval $\mathcal{K}_p$, which encompasses the time-steps k in the start-up interval:

$$g^{\text{on}}_{ipt} \leq \sum_{r \in \mathcal{R}} w_{ipr} - g^{\text{active}}_{i,p,t-k}, \quad i \in \mathcal{I},\ p \in \mathcal{P}^{\text{therm}},\ t \in \mathcal{T}_s,\ s \in \mathcal{S},\ k \in \mathcal{K}_p \setminus \{t, \ldots, sT\}. \tag{21}$$

2.2 The Consensus Loop

When the investment problem has been solved for the 26 2-week segments, information on investments in different types of generation, transmission, and variation management capacity in each 2-week segment is collected to form one capacity–cost curve per technology and region. The investments form the basis for the investment cost in the subsequent solve. The cost of the capacity that is invested in all 26 2-week segments is weighted by 1/26; however, if, for example, only k 2-week segments have made the investment, the capacity is weighted by $1/k$'th of the investment cost for all 2-week segments in the next iteration. In the initial solve, all 2-week segments share the investment cost equally, i.e., the capacity is weighted by 1/26. Below we present the construction of capacity–cost curves for generation technologies. An analogous construction for transmission technologies has also been made.

The capacity–cost curves are composed by 26 steps, where the length of the first step corresponds to the capacity investment level that is common to all 26 2-week segments. The length of the second step represents the capacity investment additional to the first step shared by all the 2-week segments except one, and so on. In order to determine the lengths of the steps, the number R_{ips} of 2-week segments that have lower or equal levels of installed capacity of technology p in region i than the 2-week segment s is calculated as[1]

[1] The *Iverson bracket* [27] returns 1 if the expression within the brackets is true; otherwise it returns 0.

$$R_{ips} = 1 + S - \sum_{u \in \mathcal{S}} [w_{ipu} \leq w_{ips}], \qquad i \in \mathcal{I},\ p \in \mathcal{P},\ s \in \mathcal{S},$$

where $\mathcal{S}$ is the set of 2-week segments. It follows that the length of the first step in the capacity–cost curve M^{e}_{i,p,r_1} is given by

$$M^{\mathrm{e}}_{i,p,r_1} = \frac{\sum_{s \in \mathcal{S}} [R_{ips} = 1] w_{ips}}{\sum_{s \in \mathcal{S}} [R_{ips} = 1]}, \qquad i \in \mathcal{I},\ p \in \mathcal{P}, \tag{22}$$

where r_1 is the first element in the set of cost classes $\mathcal{R}$. The lengths of the subsequent steps in the capacity–cost curve are calculated sequentially as

$$M^{\mathrm{e}}_{i,p,r_m} = \frac{\sum_{s \in \mathcal{S}} [R_{ips} = m] w_{ips}}{\sum_{s \in \mathcal{S}} [R_{ips} = m]} - \sum_{n=1}^{m-1} M^{\mathrm{e}}_{i,p,r_n}, \qquad i \in \mathcal{I},\ p \in \mathcal{P},\ m \in \{2, \ldots, |\mathcal{R}|\}. \tag{23}$$

The length of the last step in the capacity–cost curve is set to be very large, i.e., three times the maximum annual load in the respective region. The height of each step in the capacity–cost curve, i.e., the weight of the investment, is given by the number of 2-week segments sharing the investment, as

$$\lambda^{\mathrm{e}}_{i,p,s,r_m} = \frac{1}{S - (m-1)}, \qquad m \in \{1, \ldots, |\mathcal{R}|\}. \tag{24}$$

This cost is slightly modified in two ways: 1) the cost share is lower in the first iterations in order to enable the capacity with a high investment cost to stabilize before extinction, and 2) the cost share is lower for those 2-week segments that have not invested in the capacity that other 2-week segments have. This "rebate" is then reduced with the iteration number. Hence, it holds that

$$\lambda^{\mathrm{e}}_{i,p,s,r_m} = \frac{\alpha_{nips}}{S - \beta_n (m-1)}, \qquad m \in \{1, \ldots, |\mathcal{R}|\},\ i \in \mathcal{I},\ p \in \mathcal{P},\ s \in \mathcal{S},\ n \in \{1, \ldots, 10\}, \tag{25}$$

where the choices for the parameters α_{nips} and β_n in each iteration n are listed in Table 1. The parameter α_{nips} can take on a high ($\alpha^{\mathrm{high}}_{nips}$) or low ($\alpha^{\mathrm{low}}_{nips}$) value depending on whether or not investments have been made for the corresponding region, technology, and 2-week segment (i, p, s).

The construction of the capacity–cost curve is summarized in Algorithm 1 and illustrated for a small instance in Fig. 2.

Algorithm 1 Creating the capacity–cost curve

1: Create a list L of the capacities such that $L := (w_{ip1}, w_{ip2}, \ldots, w_{ipS})$
2: Sort the list L in ascending capacity size order. Each unique element represents a step in the capacity–cost curve.
3: The height of each step in the capacity–cost curve, i.e., $\lambda^{\mathrm{e}}_{ipr_s}$, is determined by the number of 2-week segments sharing the investment. For each element, the number of 2-week segments sharing the investment corresponds to S reduced by the order of the element in the list L.
4: **if** $\exists$ duplicates in list L **then**
    remove duplicates from the list L
5: The length of the steps corresponds to capacities, such that each new step occurs at the values present in the reduced list $L*$. The potential of each cost class, M^{e}_{i,p,r_m}, is given by the capacity in the capacity–cost curve reduced by the capacity of the prior step.

Table 1 Parameter values used in the consensus loop

Iteration number (n)	$\alpha_{nips}^{\text{low}}$	β_n	$\alpha_{nips}^{\text{high}}$
1	0.5	0.5	0.1
2	0.6	0.6	0.1
3	0.7	0.7	0.2
4	0.8	0.8	0.2
5	0.8	0.9	0.3
6	0.8	1.0	0.4
7	0.8	1.0	0.5
≥ 8	0.8	1.0	0.6

2.3 Yearly Linkages

In traditional electricity system investment models, the represented years are linked by the investment variables. The H2D model disregards any possible influence that future years might have on investments, based on the hypothesis that investments are made only to meet exactly the demand for electricity in the cost-optimal system, largely ignoring future needs in terms of capacity. This hypothesis is tested in the evaluation when the results are compared to the model with connected time.

w_1= 20, w_2= 40, w_3= 100, w_4= 55, w_5= 40, w_6= 80,
L={w_1, w_2, w_3, w_4, w_5, w_6}
sorted L={w_1, w_2, w_5, w_4, w_6, w_3}

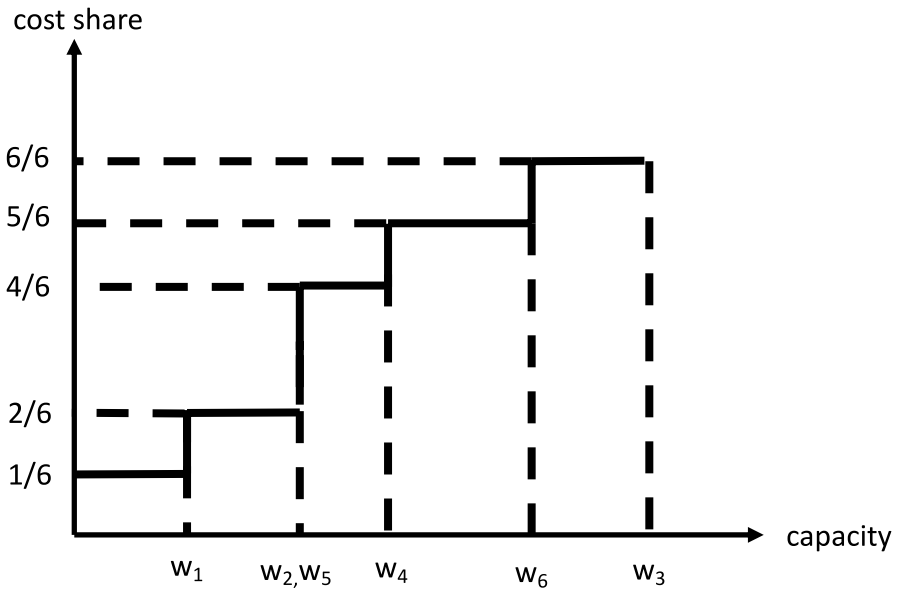

Fig. 2 An example of a capacity–cost curve

The cost of CO_2 emissions, investment costs (due to learning), efficiencies and discount rate can change between years and may influence the investment decision. For scenarios with gradually increasing costs for generation capacity or operation over the years, this increase is likely to impact investments and needs to be transferred to prior years. Electricity generation technologies that rely on fossil fuels are, for example, typically subject to a gradual increase in operational costs over the decades considered, which reduces the cost-competitiveness of these technologies in the long-term perspective. Assuming that the total cost for investments and operation of a power plant is evenly distributed across all of its hours of operation, some of the operational costs from later years need to be shifted to earlier years. The net present value of these future operational cost (with interest rate δ) is added to the objective function. Thus, we define the additional operational costs, C^{add}_{pty}, as

$$C^{\text{add}}_{pty} := \frac{1}{Z_p} \sum_{n=y}^{y+Z_p} \frac{1}{(1+\delta)^{(n-y)}} (C^{\text{run},n}_{pt} - C^{\text{run},y}_{pt}), \qquad p \in \mathcal{P},\ t \in \mathcal{T}_s,\ s \in \mathcal{S},\ y \in \mathcal{Y}, \tag{26}$$

where y is the year considered, i.e., the year in which investments are made, and Z_p is the lifetime of technology p. The costs (26) are added to the running cost C^{run}_{pt}, in the objective function (1)–(4) for the respective year.

2.4 Evaluation

All the computations are done in GAMS using CPLEX on a system with 32 cores, and 256 GB RAM. The CPLEX solver was set to deploy the barrier algorithm. The H2D model is evaluated in terms of three aspects that are challenging to combine in electricity system investment models: (1) the ability to account for strategies to manage variations; (2) the ability to consider geographically uneven resource distribution and trade; and (3) the ability to define pathways from today into the future. The capacity mix and total system cost of the solution provided by the H2D model are compared to the respective properties of solutions derived from the electricity system investment part of the H2D model in which time is fully connected, and the adjustments used to compensate for the discretization of time are removed. For cases when several years are investigated, the net present value of future costs is considered in the model with fully connected time. In the absence of time discretization, the investigated geographic scope must be kept sufficiently narrow to retain the electricity system investment model within the boundaries of the computer capacity. Therefore, one or a small set of regions is evaluated at a time. Two regions are chosen for the evaluation: Ireland (IE), representing a region with good conditions for wind power, and central Spain (ES), representing a region with good conditions for solar power. When investigating the ability to consider an uneven distribution of resources and trade, neighboring regions are incorporated into the analysis, such that the model is applied to the UK and Ireland (regions UK1, UK2, UK3, and IE) and the Iberian Peninsula (regions ES1, ES2, ES3, ES, and PT). For these cases, investments in overhead power lines, as well as in underground (or sub-sea), cables are available. Table 2 details all the cases investigated.

Table 2 Key characteristics of the cases investigated. The cost of CO_2 is gradually increased over the year investigated, and values given in the table correspond to 2020, 2030, 2040, and 2050, respectively

Case	Geographic region (s)	Year, period	Variation management options	Transmission options	CO_2 limit [ton/year]	CO_2 cost [€/ton]
IE	Ireland	2050	—	—	0	—
ES	Central Spain	2050	—	—	0	—
IE_BAT	Ireland	2050	Flow bat + Li-ion bat	—	0	—
ES_BAT	Central Spain	2050	Flow bat + Li-ion bat	—	0	—
IE_H2	Ireland	2050	Hydrogen storage	—	0	—
ES_H2	Central Spain	2050	Hydrogen storage	—	0	—
IE_BIO	Ireland	2050	Low-cost biomass	—	0	—
ES_BIO	Central Spain	2050	Low-cost biomass	—	0	—
IE_TRADE	Ireland + UK	2050	—	OHAC + SCDC	0	—
ES_TRADE	Iberia	2050	—	OHAC + SCDC	0	—
IE_YEARS	Ireland	2020–2050	—	—	—	—
ES_YEARS	Central Spain	2020–2050	—	—	—	—
IE_YEARS_CO2	Ireland	2020–2050	—	—	—	15/40/100/400
ES_YEARS_CO2	Central Spain	2020–2050	—	—	—	15/40/100/400

Table 3 gives the eleven different types of electricity generation technologies included in the modelling of this work, including fossil and bio-based thermal generation, onshore and offshore wind power, and solar PV. Thermal generation units are aggregated based on technology type and the thermal process, including start-up time, start-up cost and minimum load level, are represented by linear approximations as suggested by [26] and evaluated by [4]. Onshore wind power is subdivided into twelve investment classes, representing sites with different wind resources. Additional generation technologies, representing, for example, different wind turbine technologies, can easily be integrated into the model structure. The costs and properties of the generation technologies are detailed in Appendix B. When evaluating the ability of the H2D model to identify pathways for the electricity system, both models are solved for one year per decade, i.e., 2020, 2030, 2040, and 2050, with a cost of CO_2 of 15, 40, 100, and 400 €/MWh, respectively. An interest rate of 5% is applied throughout the work.

The ability to account for strategies to manage variations is tested by offering three types of variation management to the model: (1) the possibility to invest in

Table 3 Generation and storage technologies included in the modelling of this work and their abbreviations

Abbreviation	Technology
Coal ST	Coal steam turbine
NG CCGT	Natural gas combined cycle gas turbine
NG GT	Natural gas open cycle gas turbine
Biomass ST	Biomass steam turbine
Biogas CCGT	Biogas combined cycle gas turbine
Biogas GT	Biogas open cycle gas turbine
Bio-coal CCS	Bio-coal steam turbine with carbon capture and storage
Nuclear	Nuclear power
Solar photovoltaics	Solar PV
Onshore wind	Onshore wind power
Offshore wind	Offshore wind power
BAT	Lithium-ion battery
H2	Lined rock underground hydrogen storage

Li-ion batteries and flow batteries; (2) access to low-cost biomass (i.e., 30 €/MWh instead of 40 €/MWh); and (3) the generation and storage of hydrogen. In the hydrogen storage case, a constant hydrogen demand is added exogenously to the model such that the annual electricity demand is increased by 20%, and investments in hydrogen storage and additional electrolyzer capacity are made available. The costs and properties of the variation management technologies are listed in Appendix B.

For a fair comparison of the total system costs, the investments in electricity generation capacity provided by the H2D model were fixed in the electricity system investment model with connected time, and the total system cost of the solution of the H2D model was accepted as provided by the model with connected time. Investments in hydrogen storage capacity provided by the H2D model is not transferred to the model with connected time, since the low cost of this storage makes it suitable for seasonal storage which the H2D model does not aspire to account for.

3 Results

The capabilities of the H2D model to account for variation management, uneven distribution of resources and trade, and yearly linkages are evaluated in this section. The section ends with an evaluation of model run times. However, prior to the evaluation, the model is tested for convergence. Figure 3 gives the share of installed capacity which is different in the H2D solution compared to the least-cost solution provided by the model with connected time, for each iteration. As the figure shows, this share is consistently reduced for up to 10 iterations, after which the installed capacity provided by the H2D model stabilizes and remains stable for the next 40 iterations. Based on this test, subsequent model runs iterate the consensus loop ten

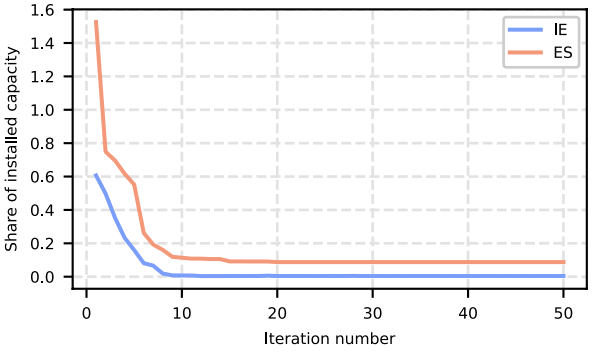

Fig. 3 The share of the installed capacity which is different in the H2D solution as compared to the least-cost solution provided by the corresponding model with connected time

times. For the IE region, the share of installed capacity, which differ between the H2D solution and the least-cost solution, is 0.7% after ten iterations and subsequently plateaus at 0.4%. For the ES region, the share of installed capacity, which differ between the H2D model and the least-cost solution, is 8.8%. However, after inspection, the difference in installed capacity in the ES region is mainly due to differences in investments between the different wind classes.

Figure 4 gives the increase in costs to meet the demand for electricity if the H2D solution is applied instead of the least-cost solution provided by the model with connected time. As the figure shows, the solution provided by the H2D model is less than 1.12% more expensive than the least-cost solution. Among the variation management strategies investigated, the impact of batteries on the cost-optimal system composition is the most challenging to capture. Including the investment in battery capacity in the cost-optimal system composition, the total system cost is around 1% higher for the system suggested by the H2D model than for the system suggested by the model in which time is connected for both regions investigated. The total system cost of the H2D solution is also around 1% higher than the least-cost solution for the cases in which several regions are considered. Another challenging case for the H2D model is when several years are connected and there is a gradual change in policy between the years, which in this work is exemplified by a gradually increasing cost of CO_2. The following sections analyze the differences in system composition for

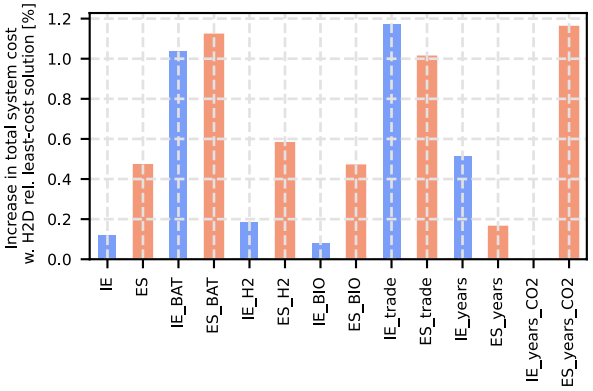

Fig. 4 Increase in the total system cost with the H2D solution relative to the least-cost solution provided by the model with connected time for the cases investigated

the cases investigated, in order to explain the higher total system cost of the H2D solution relative to the least-cost solution and interpret the results provided by the H2D model.

3.1 Ability to Account for Strategies to Manage Variations

The key motivation for using the H2D model is that it provides a tool that allows accounting for the impact of strategies to manage variations on the electricity system composition in wind-dominated systems. Figure 5a gives the installed capacity in the IE system, with the requirement that CO_2 emissions are avoided, as given by the model that involves connected time. One by one, hydrogen demand and storage, batteries, and low-cost biomass are introduced into the system. As shown in Fig. 5a, the demand for hydrogen is mainly met by additional investments in wind power in the IE region.

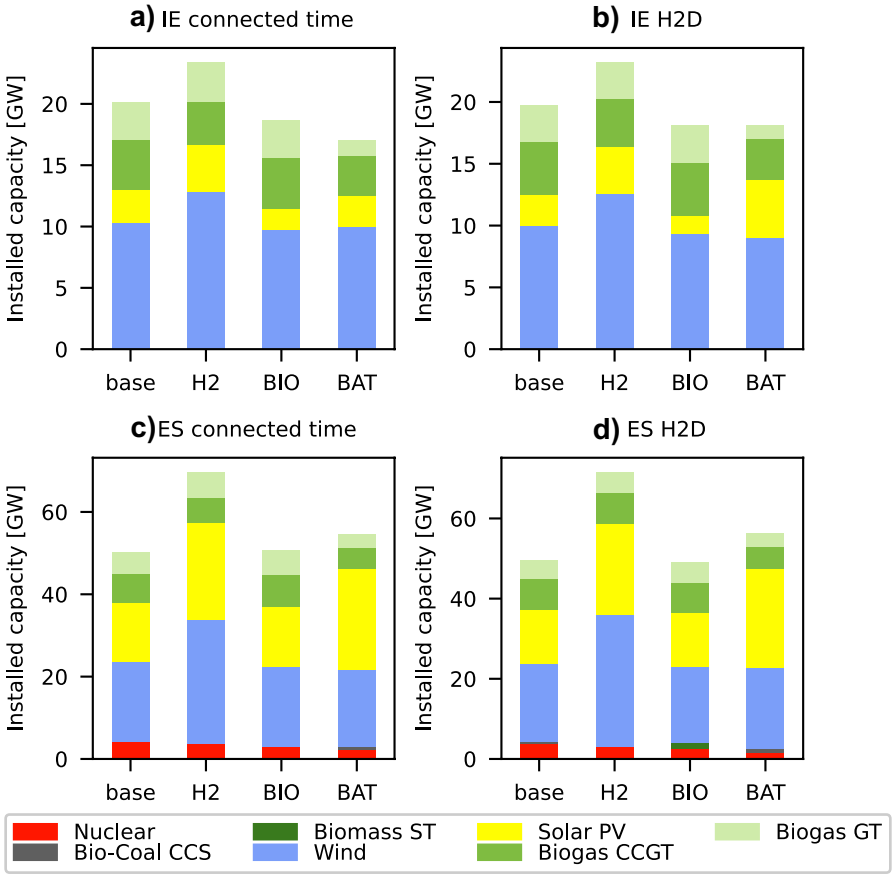

Fig. 5 Installed capacities for **a** the IE case with connected time, **b** the IE case with H2D, **c** the ES case with connected time, and **d** the ES case with H2D, with and without variation management being available

Investments in solar PV also increase slightly, whereas investments in biogas combined cycle units and biogas gas turbines remain more or less unchanged. There is an investment in 2.97 GW of electrolyzer capacity and in 50.94 GW of hydrogen storage to meet the demand for hydrogen flexibly. Low-cost biomass competes with variable renewable electricity (vRE) in this region and reduces investments, mainly in solar PV but also slightly in wind power, while investments in biogas combined cycle units increase. Batteries have a weak impact on vRE investments in this wind-dominated region, although they reduce the need for biogas-fired peak generation.

Figure 5b reveals the installed capacities given by the H2D model, in which the investment problem is split into 2-week segments. As the figure shows, investments without the strategies to manage variations provided by the H2D model are very similar to those provided by the model with connected time. In addition, the impacts of hydrogen consumption and low-cost biomass on the installed capacity are closely mimicked by the H2D model. The investment in electrolyzer capacity given by the H2D model is 3.1 GW, which is an overestimation of 6.0%. The level of hydrogen storage suggested by the H2D model is, as expected, highly underestimated as hydrogen storage is associated with a low cost and can be applied to store hydrogen between seasons. However, the ability of the H2D model to provide a good estimate of the impact of hydrogen storage on all types of generation capacity indicates that it is the impact of the hydrogen storage on timescales of up to two weeks which mainly impact the electricity system design, rather than the system services it provides on seasonal basis. As indicated in Fig. 5, the impact of batteries on the cost-optimal system composition is the variation management strategy that is the most challenging to capture for the H2D model. This is partly due to the fact that in the case of hydrogen storage, the power rating of the storage charging (i.e., the electrolyzer capacity) is here distinguished from the sizing of the storage and the method proposed disregards the sizing of the hydrogen storage, whereas the power rating of the batteries follows from the choice of storage capacity and is dimensioned with the H2D model.

Figure 5c gives the installed capacities in the ES system, as given by the model with connected time. As the figure indicates, solar PV plays a greater role in this system compared to the IE system, and this role is enhanced by both hydrogen consumption and storage, and by batteries. Hydrogen consumption and storage is the only variation management strategy that increases the wind power capacity of the system. Figure 5d gives the system composition from the H2D model and shows that the response to variation management is very similar to that given by the model with connected time.

3.2 Ability to Account for Trade

Figure 6 shows the cost optimal system compositions for Ireland and the UK, as given by the model with connected time (a), by the H2D model (b), and the corresponding figures for the Iberian Peninsula (c and d). The introduction of trade suggests many more solutions that are almost equivalent in terms of total system cost, in particular if the regions are similar and the cost of trade is low. The differences in installed capacity between the solution given by H2D model (Fig. 6b) and the model with connected time (Fig. 6a) are larger compared to the single-region cases.

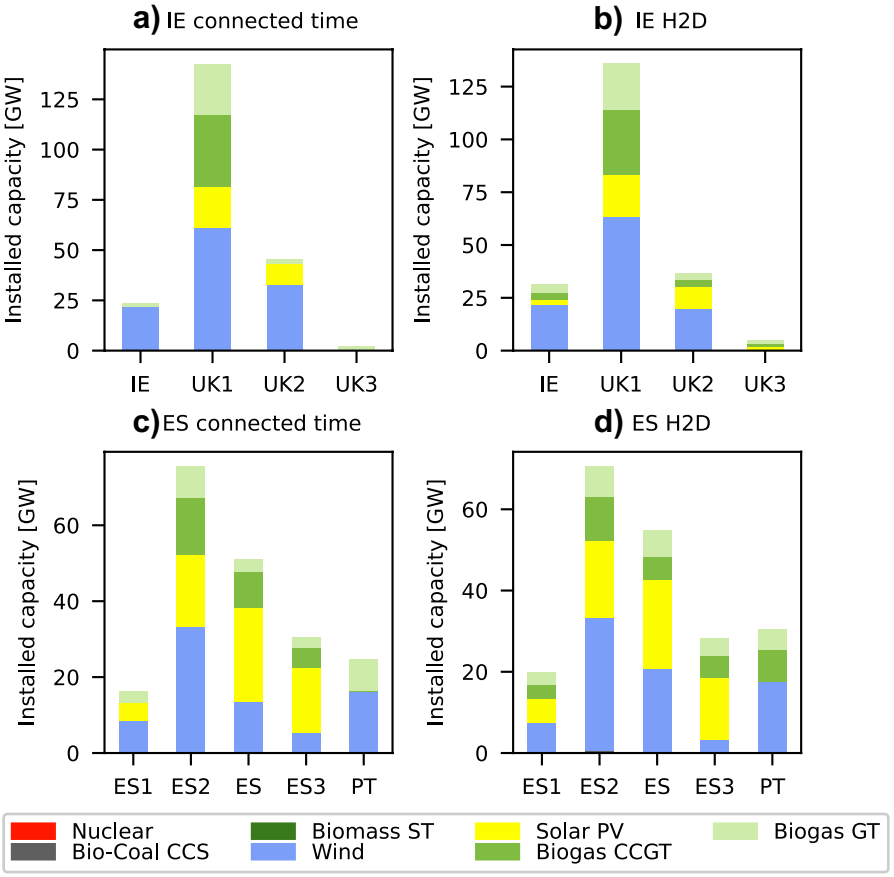

Fig. 6 The installed capacities for **a** the IE-trade case with connected time, **b** the IE-trade case with H2D, **c** the ES-trade case with connected time, and **d** the ES-trade case with H2D

Moreover, investments in transmission capacity vary considerably between the solutions provided by the H2D model and the fully connected model. The differences between the solutions are attributed to slight differences in wind and solar resources between the neighboring regions, and the option to invest in the region with best resources and transmission capacity or settle for slightly worse resources and avoid transmission capacity investments. However, if the generation capacities of the individual regions are summed, the results provided by the two models are again very similar and the total cost of the H2D solution is at the most 1.1% above the least-cost solution for the regions investigated.

3.3 Ability to Account for Yearly Linkages

Figure 7 shows the investments in new capacity in the IE and ES systems over time when they are subject to an increasing cost for CO_2. The corresponding figure without

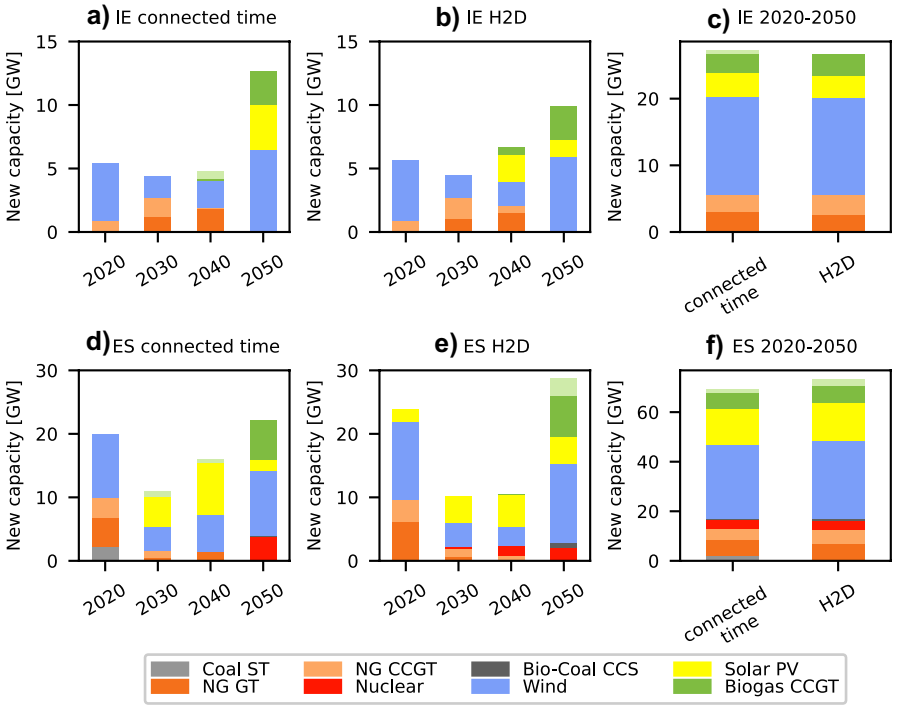

Fig. 7 The installed capacities for **a** the IE-years-CO2 case with connected time, **b** the IE-years-CO2 case with H2D, and **c** the years 2020–2050 for the two IE cases compared, **d** the ES-years-CO2 case with connected time, **e** the ES-years-CO2 case with H2D, and **f** the years 2020–2050 for the two ES cases compared

a cost for CO_2 can be found in Appendix C. This is a brown-field case, with existing generation capacity as given by Kjärstad and colleagues [28] as the starting point. Figure 7b, d shows the investments in generation capacity for the four decades considered by the H2D model, and it can be seen that the reallocation of running costs between years, as presented in the methodology section, prevents investments in coal-fired generation and also late investments in natural gas-fired generation. However, comparing the investments given by the H2D model to those given by the model with connected time, there are clear visual differences in both the IE and ES cases, indicating that investments in electricity generation associated with CO_2 emissions are faced out slightly too fast with the approach applied in the H2D model. There is an additional difference between the solutions provided by the two models related to the timing of solar PV investments, which are made earlier in the H2D model than in the model with connected time. This is the case because the model with connected time has information that the investment costs of solar drastically decline (exogenously) over time. However, it can be argued that the myopic H2D model better reflects the behaviors of wind and solar PV investors for whom future cost reductions are uncertain. Figures 7c and 7f compare the total investments over the years investigated, as given by the two models and reveals that, overall, the difference in investments is very small.

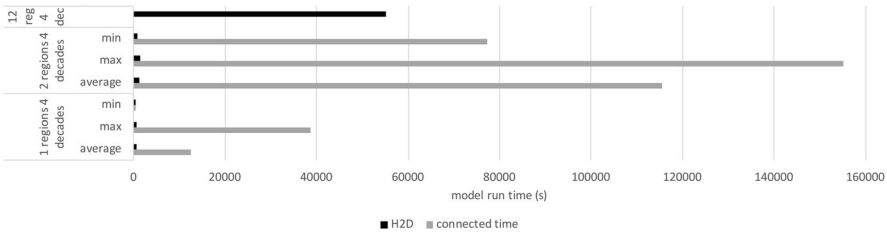

Fig. 8 Model run times for the model with connected time and the H2D model when applied to problems covering several regions and years

3.4 Computing Time Requirements

Although the accuracy of the model can be evaluated by tests limited in geographical and temporal scope, the motivation for decomposing the capacity expansion problem is first evident when several geographical regions and multiple years are considered. Figure 8 gives the model run times for the model with connected time and the H2D model when applied to a problem covering 1, 2, and 12 regions. Results are based on model runs for Germany, the UK, Sweden and Poland, except for the 12 region case which was only performed with the H2D model for one set of regions (northern Europe). All cases have temporal scope of four decades, represented by one year per decade, and a three-hour time resolution. Furthermore, all cases apply a low cost for biomass (i.e., 30 €/MWh) and include the possibility to invest in batteries and hydrogen storage. As previously stated, all model runs are carried out on a computer with 256 GB RAM and 32 CPU:s. As Fig. 8 illustrates, both models have acceptable model run times when one region is considered, and in one case the model with connected time can match the time of the H2D model. However, when two regions are considered, the run time for the model with connected time rises dramatically to levels corresponding to between one and two days, while the run time for the H2D model is less than half an hour. It is found that the H2D model solves the capacity expansion problem for northern Europe, here represented by twelve regions including all regions considered in the 2-region model runs, in fifteen hours.

4 Discussion

The method proposed in this paper applies a parallel computing approach to solve the electricity system capacity expansion problem, thereby efficiently reducing computer memory requirements. The method is also shown to reduce calculation times, although the extent of this reduction depends on the computer and problem properties. In contrast to the now widely applied representative days method, the method proposed here discretizes time into 2-week periods rather than days, to ensure the capture of high-wind and low-wind events that last several days. The 2-week segments cover the cycling of thermal generation and hydrogen storage as responses to wind variability. For electricity systems dominated by variability on

other timescales, the method proposed can be applied to discretize the time dimension into segments of any number of weeks. It should be noted, though, that longer week segments result in lower resolution of the capacity–cost curves in the consensus loop and may therefore reduce the accuracy of the method.

One drawback of the method proposed here is that it cannot dimension seasonal storages. While the operation of seasonal storage can likely be captured well, as all hours (or every third hour in this work) of the year are represented, this remains to be proven. However, from the present work, it can be observed that energy storage between 2-week segments (captured with the fully connected time model but not with the H2D model) has a low impact on the cost-optimal system composition for the cases investigated. This indicates that seasonal storage capacity could be dimensioned in a post-process.

The proposed method offers the possibility to solve large capacity expansion problems on normal computers, since model segments can be solved independently after one another. However, the method is preferably applied to a computer or a cluster with a large number of CPUs (ideally, 26 or more) to achieve an efficient reduction in model run time.

The modelling methodology proposed targets the challenging combination of wind variation management and trade in electricity system investment models. If wind power or trade is not of relevance for the region investigated, representative days or time-slicing is likely more efficient modelling methodologies.

5 Conclusion

The Hours-to-Decades model, which is an electricity system investment model that is designed to account for strategies to manage wind power variations, is presented and evaluated. The model maintains chronology in time within 2-week segments, thereby providing a detailed description of the ways in which wind power variations, with a typical duration of several days, are accommodated by the electricity system. Instead of reducing the time, the H2D model discretizes time such that the capacity expansion problem can be solved separately for each time period. This drastically reduces the memory requirements. When utilizing computers with a number of CPUs or computer clusters, the H2D model reduces model run times drastically compared to a model with fully connected time.

When evaluated for one region with very good wind resources and for one region with very good solar resources, the model is found to provide solutions for which the total system cost is no more than 1.12% higher than for a model with connected time. Accuracy is retained, even if the system is exposed to a range of strategies to manage variations.

Appendix

A Nomenclature

Tables 4, 5, and 6 list the index sets, the variables, and the parameters, respectively, used in the electricity system model.

Table 4 The index sets used in the electricity system model

Symbol	Representation	Member
$\mathcal{I}$	set of all regions	i, j
$\mathcal{P}$	$:= \mathcal{P}^{\text{bat}} \cup \mathcal{P}^{\text{electrolysis}} \cup \mathcal{P}^{\text{hydrogen}} \cup \mathcal{P}^{\text{gen}}$; set of all technology aggregates	p
$\mathcal{P}^{\text{bat}}$	set of all battery technologies	p
$\mathcal{P}^{\text{electrolysis}}$	set of all electrolyzer technologies	p
$\mathcal{P}^{\text{hydrogen}}$	set of all hydrogen storage technologies	p
$\mathcal{P}^{\text{gen}}$	$:= \mathcal{P}^{\text{wind}} \cup \mathcal{P}^{\text{therm}} \cup \mathcal{P}^{\text{solar}}$; set of all electricity generation technologies	p
$\mathcal{P}^{\text{wind}}$	set of all wind technologies	p
$\mathcal{P}^{\text{therm}}$	set of all thermal technologies	p
$\mathcal{P}^{\text{solar}}$	set of all solar technologies	p
$\mathcal{Q}$	set of technologies for transmission	q
$\mathcal{S}$	$:= \{1, \ldots, S\}$; set of all 2-week segments (typically, $S = 26$)	s
$\mathcal{T}_s$	$:= \{(s-1)T + 1, \ldots, sT\}$; set of all time steps in the 2-week segment $s \in \mathcal{S}$	t
$\mathcal{N}$	set of iterations	n
$\mathcal{R}$	set of cost classes, i.e., the steps in the cost–supply curve	r
$\mathcal{K}_p$	$:= \{0, \ldots\}$; set of hours in the start-up interval for technology $p \in \mathcal{P}^{\text{therm}}$	k
$\mathcal{Y}$	set of years	y

B Data

Table 7 gives the investment and variable costs for the electricity generation technologies considered in the model. The investment costs and fixed operation and maintenance costs are based on IEA World Energy Outlook 2016 [29], with the exception of the costs for onshore wind power, which are based on the costs presented by Mone et al. [30], with a yearly learning rate of 0.4%. In the model, annualized investment costs are applied assuming a 5% interest rate. Technology learning for thermal generation is included as gradual improvement in the efficiencies of these technologies, reflected as a reduced variable cost in Table 7. The variable costs listed in Table 7 exclude the cost of carbon dioxide, which vary between years. The cost of cycling thermal generation is not part of the variable cost. Instead, the start-up costs and part-load costs are included explicitly in the optimization. The start-up costs, part-load costs, and minimum load level applied here are based on the report of Jordan and Venkataraman [31], in which all the technologies that employ solid fuels use the cycling costs given for large sub-critical coal power plants. The start-up fuel is, however, changed to biogas rather than oil in all bio-based generation in the present work. The cost of carbon dioxide emissions related to starting thermal generation varies from year to year and is therefore not included in the start-up costs in Table 7. The cycling properties of nuclear power are based on the paper by Persson et al. [32] who describe a start-up time of 20h and a minimum load level of 70%. Biogas is assumed to be produced through the gasification of solid biomass, with 70% conversion efficiency. The cost of the gasifier equipment is included in the form of 20 €/MWh added to the fuel

Table 5 The variables used in the electricity system model

Symbol	Restriction	Explanation	Unit
w_{ipr}	≥ 0	investment in region $i \in \mathcal{I}$ in generation technology $p \in \mathcal{P}^{\text{gen}}$ in cost class $r \in \mathcal{R}$	GW
w_{ipr}	≥ 0	investment in storage capacity in region $i \in \mathcal{I}$, technology $p \in \mathcal{P}^{\text{bat}} \cup \mathcal{P}^{\text{hydrogen}}$ in cost class $r \in \mathcal{R}$	GWh
h_{ijqr}	≥ 0	investment in transmission capacity between regions $i, j \in \mathcal{I}$ using transmission technology $q \in \mathcal{Q}$ in cost class $r \in \mathcal{R}$	GW
g_{ipt}	≥ 0	electricity generation in region $i \in \mathcal{I}$, technology $p \in \mathcal{P}^{\text{gen}}$ at time step $t \in \mathcal{T}_s$, $s \in \mathcal{S}$	GWh/h
g_{ipt}	≥ 0	battery storage in region $i \in \mathcal{I}$, technology $p \in \mathcal{P}^{\text{bat}}$ at time step $t \in \mathcal{T}_s$, $s \in \mathcal{S}$	GWh
g_{ipt}	≥ 0	hydrogen storage in region $i \in \mathcal{I}$, technology $p \in \mathcal{P}^{\text{hydrogen}}$ at time step $t \in \mathcal{T}_s$, $s \in \mathcal{S}$	GWh
e_{ijt}		electricity export from region $i \in \mathcal{I}$ to region $j \in \mathcal{I}$ at time step $t \in \mathcal{T}_s$, $s \in \mathcal{S}$ ($e_{ijt} < 0$ represents import to i from j)	GWh/h
e^{pos}_{ijt}	≥ 0	absolute value of electricity export from region $i \in \mathcal{I}$ to region $j \in \mathcal{I}$ at time step $t \in \mathcal{T}_s$, $s \in \mathcal{S}$	GWh/h
c^{cycl}_{ipt}	≥ 0	resulting thermal cycling costs in region $i \in \mathcal{I}$ for technology $p \in \mathcal{P}$ at time step $t \in \mathcal{T}_s$, $s \in \mathcal{S}$	k€/h
b^{charge}_{ipt}	≥ 0	battery charging in region $i \in \mathcal{I}$, technology $p \in \mathcal{P}^{\text{bat}}$ at time step $t \in \mathcal{T}_s$, $s \in \mathcal{S}$	GWh/h
$b^{\text{discharge}}_{ipt}$	≥ 0	battery discharging in region $i \in \mathcal{I}$, technology $p \in \mathcal{P}^{\text{bat}}$ at time step $t \in \mathcal{T}_s$, $s \in \mathcal{S}$	GWh/h
g^{active}_{ipt}	≥ 0	activated thermal capacity in region $i \in \mathcal{I}$, technology $p \in \mathcal{P}^{\text{therm}}$ at time step $t \in \mathcal{T}_s$, $s \in \mathcal{S}$	GW
g^{on}_{ipt}	≥ 0	started thermal capacity in region $i \in \mathcal{I}$, technology $p \in \mathcal{P}^{\text{therm}}$ at time step $t \in \mathcal{T}_s$, $s \in \mathcal{S}$	GW
d^{hydrogen}_{it}	≥ 0	electricity consumption in the electrolyzer in region $i \in \mathcal{I}$ at time step $t \in \mathcal{T}_s$, $s \in \mathcal{S}$	GWh/h

Table 6 The parameters used in the electricity system model

Symbol	Representation	Unit
S	number of 2-week segments	1
T	number of time steps in each 2-week segment	1
C_p^{inv}	investment cost of technology $p \in \mathcal{P}^{\text{gen}}$	k€/GW
C_p^{inv}	investment cost of storage capacity for technology $p \in \mathcal{P}^{\text{bat}} \cup \mathcal{P}^{\text{hydrogen}}$	k€/GWh
$C_{q,i,j}^{\text{h-inv}}$	investment cost of transmission technology $q \in \mathcal{Q}$ between regions $i,j \in \mathcal{I}$	k€/GW
$\lambda_{ipsr}^{\text{e}}$	share of the investment cost for technology $p \in \mathcal{P}$ in region $i \in \mathcal{I}$ taken by cost class $r \in \mathcal{R}$ and segment $s \in \mathcal{S}$	1
α_{nips}, β_n	parameters used to compute $\lambda_{ipsr}^{\text{e}}$ in iteration n of the consensus loop	1
$\lambda_{ijqrs}^{\text{h}}$	share of the investment cost for transmission technology $q \in \mathcal{Q}$ between regions $i,j \in \mathcal{I}$ taken by cost class $r \in \mathcal{R}$ and segment $s \in \mathcal{S}$	1
C_{pt}^{run}	running cost of technology $p \in \mathcal{P}$ at time step $t \in \mathcal{T}_s$, $s \in \mathcal{S}$	k€/GWh
C_t^{exp}	cost of transmitting electricity at time step $t \in \mathcal{T}_s$, $s \in \mathcal{S}$	k€/GWh
M_{ipr}^{e}	cost class potential for generation technology $p \in \mathcal{P}$ in region $i \in \mathcal{I}$ and cost class $r \in \mathcal{R}$	GW
M_{ijqr}^{h}	cost class potential for transmission technology $q \in \mathcal{Q}$ between regions $i,j \in \mathcal{I}$ in cost class $r \in \mathcal{R}$	GW
D_{it}	demand for electricity in region $i \in \mathcal{I}$ at time $t \in \cup_{s \in \mathcal{S}} \mathcal{T}_s$	GWh/h
D_i^{hydrogen}	electricity demand for hydrogen in region $i \in \mathcal{I}$	GWh/h
η_p	efficiency of technology $p \in \mathcal{P}$	1
A_{ip}	regional resources based on land available in region $i \in \mathcal{I}$ for technology $p \in \mathcal{P}$	GW
ξ_p^{min}	minimum share of load for $p \in \mathcal{P}^{\text{therm}}$	1
C_{ipt}^{on}	start-up cost in region $i \in \mathcal{I}$ for technology $p \in \mathcal{P}^{\text{therm}}$ at time step $t \in \mathcal{T}_s$, $s \in \mathcal{S}$	k€/(GW·h)
C_{ipt}^{part}	part-load cost in region $i \in \mathcal{I}$ for technology $p \in \mathcal{P}^{\text{therm}}$ at time step $t \in \mathcal{T}_s$, $s \in \mathcal{S}$	k€/GWh
$G_{i,p,t}^{\text{active}}$	activated thermal capacity from previous iteration in region $i \in \mathcal{I}$, technology $p \in \mathcal{P}^{\text{therm}}$ at time step $t \in \mathcal{T}_s$, $s \in \mathcal{S}$	GW
$G_{i,p,t}^{\text{on}}$	started thermal capacity from previous iteration in region $i \in \mathcal{I}$, technology $p \in \mathcal{P}^{\text{therm}}$ at time step $t \in \mathcal{T}_s$, $s \in \mathcal{S}$	GW
θ_{ipt}	weather profile for region $i \in \mathcal{I}$ of technology $p \in \mathcal{P}$ at time step $t \in \mathcal{T}_s$, $s \in \mathcal{S}$	1
C_{pty}^{add}	additional, future, running cost for technology $p \in \mathcal{P}$ at time step $t \in \mathcal{T}_s$, $s \in \mathcal{S}$ and year $y \in \mathcal{Y}$	k€/GWh
Z_p	technical lifetime of technology $p \in \mathcal{P}$	years

Table 7 Costs and technical data for the electricity generation and transmission technologies. Variable 'low-cost' concerns the low-cost biomass case

Technology	Investment costs		Variable costs	Variable low-cost	Fixed O&M costs	Lifetime	Minimum load-level	Start time	Start cost
	[M€/MW]	[€/MW,km]	[€/MWh]	[€/MWh]	[k€/MW,yr]	[yr]	[share]	[h]	[€/MW]
Coal ST	1.56	—	20	20	27	40	0.35	12	250
NG CCGT	0.76	—	50	50	13	30	0.2	6	45
NG GT	0.38	—	80	80	8	30	0.5	6	0
Biomass ST	1.86	—	82.6	62.5	50	40	0.35	12	240
Biomass CCGT	0.76	—	110	89.9	13	30	0.2	6	245
Biomass GT	0.38	—	183	149	8	30	0.5	0	0
Bio-coal CCS	3.46	—	36.7	34.2	113	30	0.35	12	240
Hydropower	2.06	—	1.0	1.0	47	500	0	0	0
Nuclear	5.15	—	18.9	18.9	154	60	0.7	24	660
Solar PV	0.60	—	1.1	1.1	10	25	0	0	0
Onshore wind	1.24	—	1.1	1.1	30	25	0	0	0
Offshore wind	1.84	—	1.1	1.1	100	25	0	0	0
Transmission (OHAC)	—	0.6	0.01	0.01	—	40	0	0	0
Transmission (HVDC)	0.756	0.63	0.01	0.01	—	40	0	0	0

Table 8 Full-load hours (FLH) and maximum capacity limits (Cap) for onshore wind classes 4–12, offshore wind, and solar PV. The absence of available sites is indicated by Ø, while an unlimited availability of sites is indicated by ∞

Technology	Wind class	ES3 FLH [h]	Cap [GW]	HU FLH [h]	Cap [GW]	IE FLH [h]	Cap [GW]	SE2 FLH [h]	Cap [GW]
Onshore	4	2310	7.1	2370	7.8	Ø	Ø	2230	4.5
Onshore	5	2560	6.1	2570	2.4	Ø	Ø	2440	6.9
Onshore	6	2790	6.3	2750	1.3	Ø	Ø	2620	9.9
Onshore	7	3020	4.6	3070	2.4	Ø	Ø	2900	9.1
Onshore	8	3300	1.3	3350	0.2	Ø	Ø	3270	11.6
Onshore	9	Ø	Ø	Ø	Ø	Ø	Ø	3700	1.5
Onshore	10	Ø	Ø	Ø	Ø	4240	0.3	4120	1.7
Onshore	11	Ø	Ø	Ø	Ø	4640	13.8	4600	0.5
Onshore	12	Ø	Ø	Ø	Ø	5360	2.1	5260	0.1
Offshore	—	Ø	Ø	Ø	Ø	5360	∞	5260	∞
Solar PV	—	1770	24.7	1360	12.5	1000	9.6	1050	25.6

cost, rather than being incorporated into the investment cost of the biogas technologies, since biogas is storable, which means that the gasifier equipment may attain a much higher number of full-load hours compared to the power plant consuming the biogas. The total cost of the gasification equipment is taken from Thunman et al. [33], and 8,000 full-load hours are assumed.

The wind power generation profiles are calculated for wind turbines with low specific power (200 W/m2), with the power curve and losses proposed by Johansson et al. [34]. The wind speed input data are a combination of the MERRA and ECMWF ERA-Interim data for year 2012, whereby the profiles from the former are re-scaled with the average wind speeds from the latter (see [35–37]). The high resolution of the wind profiles from the ERA-Interim data was processed into wind power generation profiles and put together into 12 wind classes for each region, for which the full-load hours (FLH) and the maximum capacities (Cap) for classes 4–12, as well as the offshore wind and solar PV, are shown in Table 8. The wind farm density is set to 3.2 MW/(km)^2 and is assumed to be limited to 10% of the available land area, accounting for protected areas, lakes, water streams, roads, and cities [38].

Table 9 Costs and technical data for the variation management technologies

Technology	Investment cost		Efficiency		Fixed O&M costs	Lifetime
	[M€/MWh]	[M€/MW]	[%]	[k€/MWh,yr]	[k€/MW,yr]	[yr]
Battery, Li-ion	0.15	—	90	25	—	15
Battery, flow	0.18	—	70	13	—	30
Electrolyser	—	1.0	62	—	20	10
H_2 storage	0.011	—	100	—	—	30

Solar PV is modelled as mono-crystalline silicon cells installed with optimal tilt with one generation profile for each region. Solar radiation data from MERRA are used to calculate the generation with the model presented by Norwood et al. [39], including thermal efficiency losses. The full-load hours of solar PV in each region are shown in Table 8. The cost and technical data for VMSs are shown in Table 9 and based on [40]. The hydrogen storage is assumed to be of the large-scale, steel-lined cavern type.

C Additional Results

Figure 9 shows the investments in new capacity in the IE and ES systems over time without a cost for CO_2 (see Sect. 3.3).

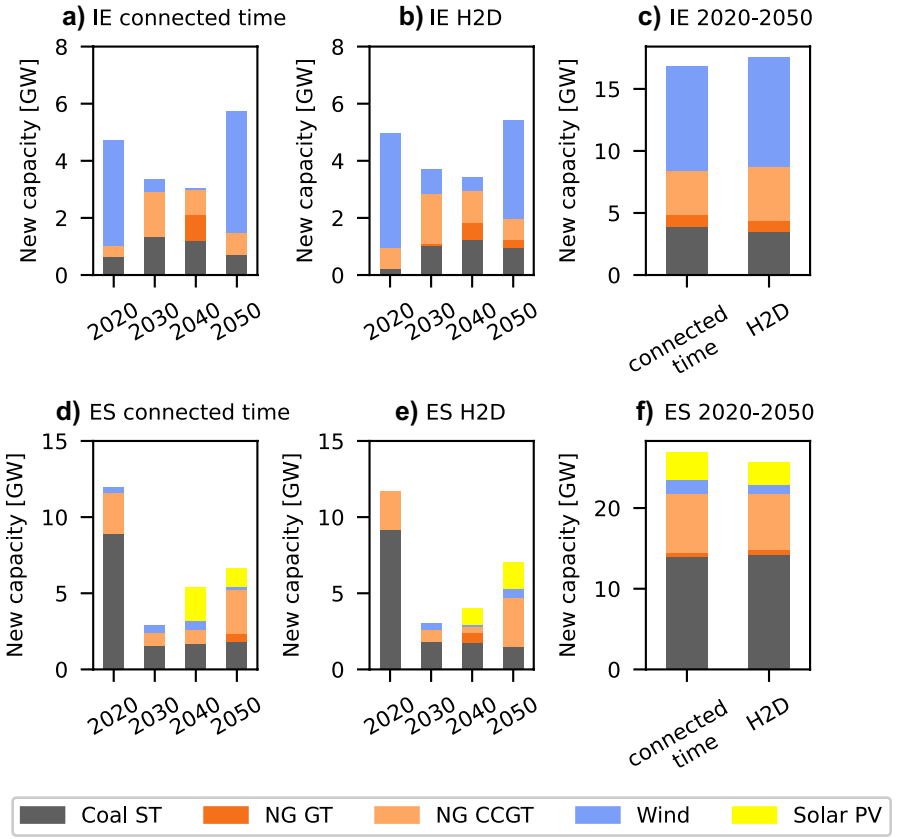

Fig. 9 The installed capacities for **a** the IE-years case with connected time and **b** the IE-years case with H2D, and **c** the years 2020–2050 for the two IE cases compared; **d** the ES-years case with connected time and **e** the ES-years case with H2D, and **f** the years 2020–2050 for the two ES-cases compared

Funding Open access funding provided by Chalmers University of Technology. The research leading to the results presented in this article was supported by the Swedish Energy Agency (grant nos. 39907-1 and 39957-1).

Data Availability The input data applied in this work are given in Appendix B together with relevant references. The datasets generated during the current study are available from the corresponding author on reasonable request.

Declarations

Conflicts of Interest On behalf of all authors, the corresponding author states that there is no conflict of interest.

References

1. IEA (2017) World energy outlook 2017. Report, International Energy Agency. URL https://www.iea.org/reports/world-energy-outlook-2017
2. Welsch M, Howells M, Hesamzadeh MR, Ó Gallachóir B, Deane P, Strachan N, Bazilian M, Kammen DM, Jones L, Strbac G, Rogner H (2015) Supporting security and adequacy in future energy systems: The need to enhance long-term energy system models to better treat issues related to variability. Int J Energy Res 39(3):377–396. https://doi.org/10.1002/er.3250
3. Pfenninger S, Hawkes A, Keirstead J (2014) Energy systems modeling for twenty-first century energy challenges. Renew Sustain Energy Rev 33:74–86. https://doi.org/10.1016/j.rser.2014.02.003
4. Göransson L (2014) The impact of wind power variability on the least-cost dispatch of units in the electricity generation system. PhD thesis, Chalmers University of Technology
5. Ringkjøb H-C, Haugan PM, Solbrekke IM (2018) A review of modelling tools for energy and electricity systems with large shares of variable renewables. Renew Sustain Energy Rev 96:440–459. https://doi.org/10.1016/j.rser.2018.08.002
6. Collins S, Deane JP, Poncelet K, Panos E, Pietzcker RC, Delarue E, Ó Gallachóir B (2017) Integrating short term variations of the power system into integrated energy system models: A methodological review. Renew Sustain Energy Rev 76:839–856. https://doi.org/10.1016/j.rser.2017.03.090
7. Haydt G, Leal V, Pina A, Silva CA (2011) The relevance of the energy resource dynamics in the mid/long-term energy planning models. Renew Energy 36(11):3068–3074. https://doi.org/10.1016/j.renene.2011.03.028
8. Wogrin S, Duenas P, Delgadillo A, Reneses J (2014) A new approach to model load levels in electric power systems with high renewable penetration. IEEE Trans Power Syst 29(5):2210–2218. https://doi.org/10.1109/TPWRS.2014.2300697
9. Lehtveer M, Mattsson N, Hedenus F (2017) Using resource based slicing to capture the intermittency of variable renewables in energy system models. Energ Strat Rev 18 https://doi.org/10.1016/j.esr.2017.09.008
10. Nahmmacher P, Schmid E, Hirth L, Knopf B (2016) Carpe diem: A novel approach to select representative days for long-term power system models with high shares of renewable energy sources. Energy 112(1):430–442. https://doi.org/10.1016/j.energy.2016.06.081
11. Mai T, Drury E, Eurek K, Bodington N, Lopez A, Perry A (2013) Resource planning model: An integrated resource planning and dispatch tool for regional electric systems. Report, National Renewable Energy Laboratory

12. Gils H-C (2016) Energy System Model REMix. Report, DLR, https://www.dlr.de/tt/Portaldata/41/Resources/dokumente/institut/system/Modellbeschreibungen/DLR_Energy_System_Model_REMix_short_description_2016.pdf
13. Gerbaulet C, Lorenz C (2017) dynELMOD: A dynamic investment and dispatch model for the future European electricity market. Technical report, Deutsches Institut für Wirtschaftsforschung (DIW), Berlin, www.diw.de; https://www.econstor.eu/bitstream/10419/161634/1/888201575.pdf
14. Frew BA, Jacobson MZ (2016) Temporal and spatial tradeoffs in power system modeling with assumptions about storage: An application of the POWER model. Energy 117:198–213. https://doi.org/10.1016/j.energy.2016.10.074
15. Tejada-Arango D, Domeshek M, Wogrin S, Centeno E (2018) Enhanced representative days and system states modeling for energy storage investment analysis. IEEE Trans Power Syst 33:6534–6544. https://doi.org/10.1109/TPWRS.2018.2819578
16. Reichenberg L, Siddiqui AS, Wogrin S (2018) Policy implications of downscaling the time dimension in power system planning models to represent variability in renewable output. Energy 159:870–877. https://doi.org/10.1016/j.energy.2018.06.160
17. Gabrielli P, Gazzani M, Martelli E, Mazzotti M (2018) Optimal design of multi-energy systems with seasonal storage. Appl Energy 219(1):408–424. https://doi.org/10.1016/j.apenergy.2017.07.142
18. Brown T, Schlachtberger D, Kies A, Schramm S, Greiner M (2018) Synergies of sector coupling and transmission reinforcement in a cost-optimised, highly renewable European energy system. Energy 160:720–739. https://doi.org/10.1016/j.energy.2018.06.222
19. Van der Hoven I (1956) Power spectrum of horizontal wind speed in the frequency range from 0.0007 to 900 cycles per hour. J Meteorol pp. 160–164
20. Guignard M, Kim S (1987) Lagrangean decomposition: A model yielding stronger Lagrangean bounds. Math Program 39(2):215–228. https://doi.org/10.1007/BF02592954
21. Larsson T, Patriksson M, Strömberg A-B (1996) Conditional subgradient optimization–Theory and applications. Eur J Oper Res 88(2):382–403. https://doi.org/10.1016/0377-2217(94)00200-2
22. Hiriart-Urruty J-B, Lemaréchal C (1993) Convex Analysis and Minimization Algorithms II: Advanced Theory and Bundle Methods, vol 306. Springer-Verlag, Berlin, Germany, p 346
23. Guignard M (2003) Lagrangean relaxation. TOP 11(2):151–228. https://doi.org/10.1007/BF02579036
24. Sørensen B (2017) Renewable Energy: Physics, Engineering, Environmental Impacts. Academic Press, Economics and Planning
25. Göransson L, Goop J, Odenberger M, Johnsson F (2017) Impact of thermal plant cycling on the cost-optimal composition of a regional electricity generation system. Appl Energy 197:230–240. https://doi.org/10.1016/j.apenergy.2017.04.018
26. Weber C (2005) Uncertainty in the electric power industry: methods and models for decision support. Springer, New York. https://www.springer.com/gp/book/9780387230474
27. Iverson KE (1962) A Programming Language. Wiley
28. Kjärstad J, Johnsson F (2007) The European power plant infrastructure–Presentation of the Chalmers energy infrastructure database with applications. Energy Policy 35(7):3643–3664. https://doi.org/10.1016/j.enpol.2006.12.032
29. IEA (2016) World energy outlook 2016. Report, International Energy Agency. https://www.iea.org/reports/world-energy-outlook-2016
30. Mone C, Hand M, Bolinger M, Rand J, Heimiller D, Ho J (2017) 2015 Cost of Wind Energy Review. Technical report NREL/TP-6A20-66861, National Renewable Energy Laboratory. https://www.nrel.gov/docs/fy17osti/66861.pdf
31. Jordan G, Venkataraman S (2012) Analysis of cycling costs in western wind and solar integration study. Report, National Renewable Energy Laboratory, Golden, Colorado, US
32. Persson J, Andgren K, Henriksson H, Loberg J, Malm C, Pettersson L, Sandström J, Sigfrids T (2012) Additional costs for load-following nuclear power plants—Experiences from Swedish, Finnish, German, and French nuclear power plants. Report 12:71, Elforsk, Stockholm, Sweden
33. Thunman H, Gustavsson C, Larsson A, Gunnarsson I, Tengberg F (2019) Economic assessment of advanced biofuel production via gasification using cost data from the GoBiGas plant. Energy Science and Engineering 7:217–229. https://doi.org/10.1002/ese3.271
34. Johansson V, Thorson L, Goop J, Göransson L, Odenberger M, Reichenberg L, Taljegård M, Johnsson F (2017) Value of wind power–Implications from specific power. Energy 126:352–360. https://doi.org/10.1016/j.energy.2017.03.038
35. ECMWF (2010) ERA-Interim u- and v-components of horizontal wind, surface solar radiation downward, skin temperature. Web Page Access Date: 2010-10-10, European Centre for

Medium-Range Weather Forecasts. https://www.ecmwf.int/en/forecasts/datasets/browse-reanalysis-datasets
36. Lucchesi R (2012) File specification for MERRA products, GMAO Office Note No. 1. Report, Global Modeling and Assimilation Office, NASA. URL http://gmao.gsfc.nasa.gov/pubs/office_notes
37. Olauson J, Bergkvist M (2015) Modelling the Swedish wind power production using MERRA reanalysis data. Renew Energy 76:717–725. https://doi.org/10.1016/j.renene.2014.11.085
38. Nilsson K, Unger T (2014) Bedömning av en europeisk vindkraftpotential med GIS-analys. Report, PROFU
39. Norwood Z, Nyholm E, Otanicar T, Johnsson F (2014) A geospatial comparison of distributed solar heat and power in Europe and the US. PLoS One 9(12):1–31. https://doi.org/10.1371/journal.pone.0112442
40. Energistyrelsen (2012) Generation of electricity and district heating, energy storage and energy carrier generation and conversion: Technology data for energy plants. Report, Energistyrelsen, Copenhagen V, Denmark. ISBN: 978-87-7844-931-3

Authors and Affiliations

Lisa Göransson[1] · Caroline Granfeldt[2] · Ann-Brith Strömberg[2]

Caroline Granfeldt
cargranf@chalmers.se

Ann-Brith Strömberg
anstr@chalmers.se

[1] Department of Space, Earth and Environment, Chalmers University of Technology, Gothenburg, Sweden

[2] Department of Mathematical Sciences, Chalmers University of Technology and University of Gothenburg, Gothenburg, Sweden